THE JOURNAL OF PHYSICAL CHEMISTRY B

ARTICLE

pubs.acs.org/JPCB

Conformation and Dynamics of 18-Membered Hexathiametacyclophanes: A Two Step Racemization as Studied by Deuterium NMR in Chiral Lyotropic Liquid Crystals

Philippe Lesot,*[,†] Christie Aroulanda,[†] Philippe Berdagué,[†] Herbert Zimmermann,[‡] and Zeev Luz*[,§]

[†]RMN en Milieu Orienté, ICMMO, UMR CNRS 8182, Université Paris Sud 11, Bât. 410, F-91405 Orsay cedex, France

[‡]Max-Planck-Institüt fur Medizinische Forschung, Jahnstrasse 29, DE-69120 Heidelberg, Germany

[§]Chemical Physics Department, The Weizmann Institute of Science, Rehovot 7100, Israel

Supporting Information

ABSTRACT:

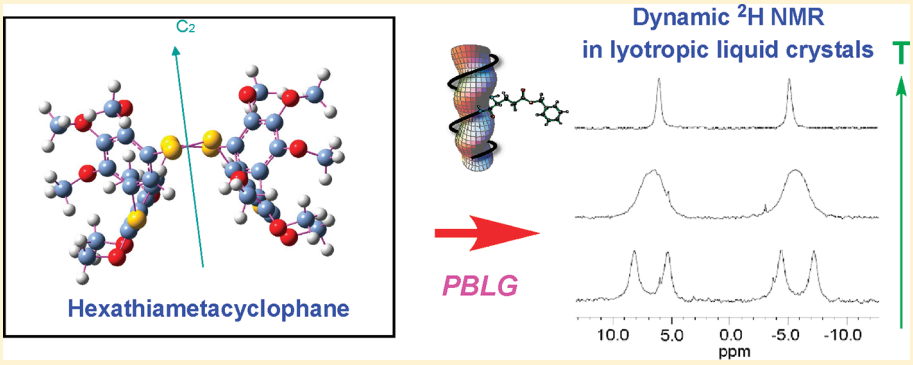

The conformation and interconversion dynamics of two derivatives of the 18-membered hexathia metacyclophane **1** and **2** were studied by ^{1}H NMR spectroscopy in isotropic solvents and by ^{2}H NMR in chiral liquid crystalline (CLC) solutions, as well as by molecular structure computations. For the analysis of the dynamic effects, we made use of the concepts of "average symmetry" and "isodynamic groups", introduced by Altmann (Altmann, *Proc. R. Soc.* **1967**, *184*, A298). Compound **1**, which is unsubstituted in the inner aromatic site, has, according to the NMR and molecular force field calculations, a boat shaped ground conformation with C_2 symmetry. It is highly flexible and in the NMR spectrum exhibits two successive dynamic processes. There is a low temperature (170−210 K, E_a = 10.5 kcal/mol) alternate "wing flipping", which corresponds to interchange between pairs of enantiomers and results, in the fast exchange limit, in an average prochiral molecule with C_{2v} symmetry. This process is followed, at higher temperatures (290−320 K, E_a = 28.5 kcal/mol), by an umbrella flipping type inversion with an average structure of D_{2h} symmetry. This second process involves averaging of effective enantiotopic into homotopic sites and can only be studied in chiral solvents. The origin of the chiral discrimination and of their stepwise averaging is discussed. Compound **2**, which is substituted with methoxy groups at the inner sites of the benzene rings, is much less flexible and exhibits dynamic effects in the NMR spectrum only at temperatures above 370 K. We were able to study the kinetic parameters of this process in isotropic solvents (E_a = 21.4 kcal/mol). As for **1**, the detailed mechanism of this process can in principle be established using dynamic NMR in CLC; however, experimental limitation precluded us from doing so. Possible alternatives and their effect on the 1D and 2D exchange spectra in CLC are discussed in a concluding section.

1. INTRODUCTION

The structural and dynamic properties of macrocyclic molecules depend delicately on their size, substitution pattern, and nature of their linking groups.[1] Often they are highly flexible and their NMR spectra in solution then correspond to average over several conformations, hampering their quantitative interpretation. Additional information beyond the temperature dependence of the NMR spectrum is then usually required. Theoretical structure computations are often helpful in this respect. Another tool, which is not often used, involves recording NMR spectra in chiral solvents. Such spectra may reveal extra information on the symmetry of the molecules by exhibiting spectral discrimination between enantiomers in optically active molecules or between enantiotopic sites in prochiral molecules.[2−7] In certain cases special dynamic effects are only expressed when recorded in chiral solvents but not in achiral ones.[4] These (chiral differentiation)

Received: June 24, 2011
Revised: September 6, 2011
Published: September 06, 2011

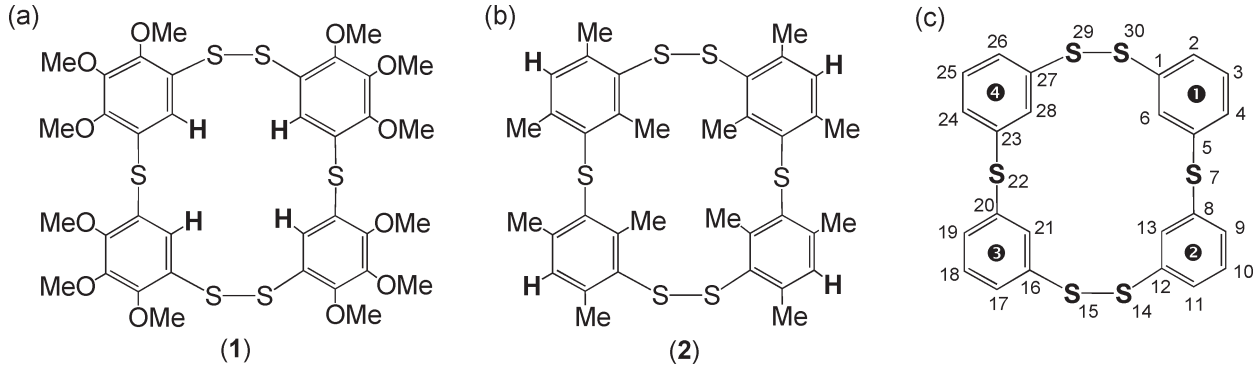

Figure 1. Molecular structures of compounds **1** (a) and **2** (b), along with the atomic numbering used for the hexathiametacyclophane ring (c). Derivatives **1** and **2**, deuterated in the unsubstituted aromatic positions, are referred to as **1-d$_4$** and **2-d$_4$**, respectively.

effects are usually more pronounced in ordered chiral solvents such as chiral liquid crystals (CLC) than in chiral isotropic solvents. This is so because of the extra anisotropic interactions which affect the NMR spectra in liquid crystals but are averaged out in isotropic solvents. Particularly useful in this respect is deuterium NMR, where the spectra exhibit quadrupolar splittings that readily lend themselves to stereochemical and dynamic studies.[8]

As specific examples we shall consider the derivatives **1** and **2** of the 18-membered macrocyclic hexathiametacyclophane ring (see Figure 1). Their structure and conformational dynamics in solution has been a source of some controversy.[9,10] The earlier work of Pappalardo et al.[10] on compound **2**, based on its ^{1}H high resolution NMR spectrum in nitrobenzene at 423 K (single aromatic peak and three methyl lines), was interpreted as due to a (4-fold) symmetric rigid crown conformation. A similar spectrum was observed for compound **1** at room temperature. However, cooling to below 220 K (in THF) resulted in gradual line broadening and eventual doubling of the spectrum with (below 180 K) two aromatic and six methyl peaks.[11] This indicated that the room temperature spectrum of **1**, in fact, corresponds to the fast exchange limit involving a pair of degenerate conformations but of unknown structure.

In the present work we extend the study of **1** to CLC solvents, using proton decoupled deuterium (^{2}H-{^{1}H}) NMR of a specifically deuterated isotopologue. The results reveal a high-temperature process, beyond that detected earlier by ^{1}H NMR,[11] which involves averaging of chiral sites. This process does not affect the ^{1}H NMR spectrum in achiral solvents, and thus demonstrates the power of using chiral (in particular CLC) solvents for dynamic studies that are not expressed in the spectra of achiral solvents.

As oriented media we used solutions of optically pure as well as racemic mixtures of poly(γ-benzylglutamate) in organic cosolvents. In the proper concentration range, such solutions form weakly ordered, chiral or achiral, lyotropic liquid crystals, highly suitable for high-resolution NMR measurements over fairly wide temperature ranges (depending on the cosolvent). These systems have been widely used and their application has been extensively reviewed in the literature.[7,8,12]

The ^{1}H NMR spectrum of **2** was originally only measured at 423 K due to its low solubility at room temperature.[11] With the higher sensitivity of present days spectrometers, we were able to record its spectrum at room temperature, where it was found to exhibit a line doubling like that found for **1** below 180 K, suggesting a similar averaging process but shifted to much higher temperatures. In the present work the kinetic parameters of this process were determined in the isotropic solvent, nitrobenzene, in the temperature range 370−410 K. Its detailed mechanism could, however, not be established from the ^{1}H NMR spectra alone. As the process involves chiral averaging, its mechanism could, in principle, be studied using CLC, as for **1**. Unfortunately, due to the limited temperature range of our cryogenic NMR probe (required for the weakly soluble **2**) we were unable to carry out such experiments. Instead, we show how the different mechanisms will be expressed when such experiments become possible.

2. EXPERIMENTAL SECTION

Material. According to the numbering system shown in Figure 1c, compounds **1** and **2** are referred to as 1,2,9,16,17,-24-hexathia[2.1.2.1]-4,5,6,11,12,13,19,20,21,26,27,28-dodecamethoxymetacyclophane and 1,2,9,16,17,24-hexathia[2.1.2.1]-4,6,8,11,13,15,19,21,23,26,28,30-dodecamethylmetacyclophane, respectively. Isotopically normal **1** was prepared according to ref 9 by reacting of 1,2,3-trimethoxybenzene with sulfurdichloride (SCl_2) in acetonitrile at room temperature (m/z = 856). Compound **1**, deuterated in the unsubstituted aromatic positions, **1-d$_4$**, was prepared from **1** by exchange in boiling CF_3COOD for 48 h (m/z = 860). Isotopically normal **2** was prepared according to ref 10 by reacting mesitylene with sulfurmonochloride (S_2Cl_2) in $CHCl_3$ using iron powder as catalyst (m/z = 664). As this compound is insoluble in boiling trifluoroacetic acid its deuterated isotopologues were prepared from appropriately deuterated starting materials. Thus, compound **2** deuterated in the aromatic sites (**2-d$_4$**) was synthetised from the corresponding aromatically deuterated mesitylene. The latter was prepared by repeated exchange of mesitylene in DCl/D_2O (5%) using tantalum high pressure autoclave at 483 K for two days. Likewise, **2** perdeuterated in all of the methyl groups (**2-d$_{36}$**) was prepared from the corresponding methyl-deuterated mesitylene. The latter was obtained from isotopically normal mesitylene by repeated exchange in D_2O with Pt/carbon (10%) at 300 °C in a high pressure stainless steel autoclave for 5 days, followed by workup, distillation, and backexchanging the aromatic deuterons with HCl/H_2O, as above.

Liquid Crystals Samples. Achiral and chiral lyotropic solvents were prepared by dissolving respectively racemic mixtures of PBLG/PBDG (referred to as PBG) or the optically active PBLG

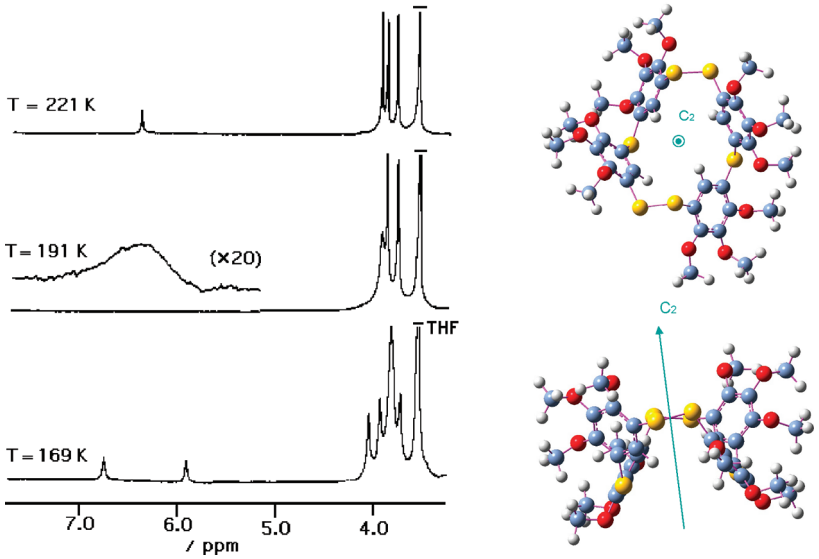

Figure 2. (a) ^{1}H 270 MHz NMR spectra of **1** at the indicated temperatures in deuterated THF (see ref 11). (b) The boat structures of **1** (C_2 symmetry) as calculated using the PM3 method in Gaussian 03 package. The C−S−S−C dihedral angle is equal to 85°.

Table 1. Kinetic Parameters Derived from the NMR Spectra for the Two Dynamic Processes of 1

temp. range K	symmetry of process	E_a, kcal/mol	$\Delta H^{\ddagger}$, kcal/mol	$\Delta S^{\ddagger}$, cal/mol K
290−320[a]	$C_{2v} \leftrightarrow D_{2h}$	28.5	27.9	44
170−210[b]	$C_2 \leftrightarrow C_{2v}$	10.5	10.1	7.1

[a] Data determined in this work using chiral anisotropic solvents. [b] Data from ref 11.

in the desired organic cosolvents ($CDCl_3$ or DMF). The detailed of the sample preparation are as described in refs 7, 12, and 13. The PBG/chloroform samples consisted of 470 mg of $CDCl_3$, 50 mg of PBLG, 50 mg of PBDG and 10 mg of **1-d$_4$**, or **2-d$_4$**. The corresponding PBLG/chloroform solutions had the same compositions, except that, instead of the racemic mixture of the polypeptide, 100 mg of PBLG was used. The PBG/DMF (PBLG/DMF) solutions consisted of 360 mg of DMF, 130 mg of polypeptide (racemic or optically active), and 10 mg of the deuterated probes. Note that due to the low solubility of **2** it was not completely dissolved in the solvent. The degree of polymerization was 767 (MW = 168.000) for PBLG and 914 (MW = 200.200) for PBDG.

NMR Measurements. Most ^{1}H (400.1 MHz) and ^{13}C (100.3 MHz) NMR measurements were carried out on a 9.4 T spectrometer equipped with a 5-mm QXO probe. The temperature dependence of the proton spectra in isotropic solvents was recorded at 500 MHz. The 1D and 2D ^{2}H-{^{1}H} NMR spectra in CLC were recorded at 9.4 T (61.3 MHz) with a 5-mm QXO probe, 14.1 T (92.1 MHz) with a 5-mm ^{2}H selective cryoprobe, and at 21.1 T (138.1 MHz) with a 5-mm BBO probe. The classical CPD sequence (WALTZ-16) was applied for proton decoupling when required (see the figure captions).

Computational and Dynamic Calculations. Three dimensional models of the conformers were constructed using the Builder model of the Insight II software package (Accelrys, San Diego, CA) and energy minimized using the CV force field (CVFF) with the Discover-3 module. The models were further subjected to several cycles of short molecular dynamics simulation (10 ps) followed by energy minimization in order to test their stability.[14] The in vacuo ground state conformation of the metacyclophane ring was also checked using the Gaussian 03 package and the included semiempirical PM3 method.[15]

3. RESULTS AND DISCUSSIONS

3.1. Metacyclophane 1. *3.1a. Proton NMR Spectrum in an Isotropic Solvent and the Low-Temperature Process.* The ^{1}H NMR spectrum of **1** was studied previously in THF solutions and was shown to exhibit dynamic line broadening and coalescence in the temperature range 170−210 K.[11] Examples of spectra are reproduced in Figure 2a. Below 170 K the spectrum exhibits two aromatic and six methyl peaks, suggesting that the "frozen" conformation at this temperature is 2-fold degenerate. Above 200 K the spectrum consists of a single aromatic signal and only three methoxy peaks indicating that the dynamic process "averages" the nonequivalent parts of the conformer. The rate constants for this process were determined[11] by analysis of the dynamic spectra, and the results are summarized in Table 1. For reasons explained later it is referred to as the $C_2 \leftrightarrow C_{2v}$ process.

3.1b. ^{2}H NMR Spectrum in Liquid Crystalline Solvents and the High Temperature Process. The deuterium NMR measurements in liquid crystalline solvents were performed on the **1-d$_4$** isotopologue. Examples of spectra recorded as a function of the temperature (in the range 230−360 K) in the achiral solvent PBG/$CHCl_3$ and the chiral solvent PBLG/$CHCl_3$ are shown in Figure 3, panels a and b, respectively. More detailed numerical data are included in the Supporting Information (see Figures SI-1a and SI-1b).

In the achiral solvent the spectrum consists of a single doublet. Its splitting, $\Delta\nu_Q^{PBG}$, corresponds to the average quadrupole interaction of the aromatic deuterons in the liquid crystalline solution. The fact that a single doublet is observed is consistent with the ^{1}H spectrum recorded at the high temperatures (above 220 K) in the isotropic solutions, where a single peak is observed for the aromatic hydrogens (Figure 2). The sign of the

dx.doi.org/10.1021/jp205958k |J. Phys. Chem. B 2011, 115, 11793–11804

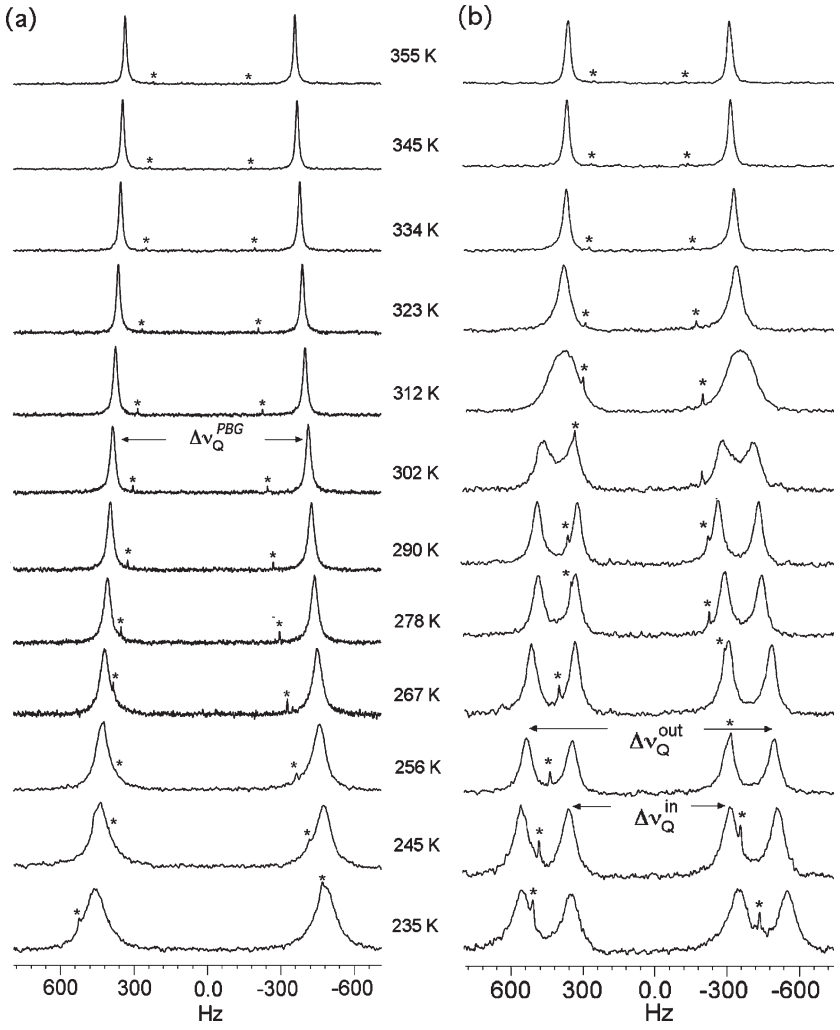

Figure 3. ^{2}H-{^{1}H} NMR spectra (61.4 MHz) of **1-d$_4$** dissolved in PBG/$CHCl_3$ (a) and in PBLG/$CHCl_3$ mesophases (b) as a function of the temperature (as indicated). A total of 512 spectra were added for each trace, with a recycling time of 1s. No digital filtering was applied. Asterisks indicate ^{2}H signals due to the natural abundant deuterium (NAD) in chloroform.

$\Delta\nu_Q$'s (as determined by comparing the C−D quadrupolar splitting with the ^{13}C−^{1}H dipolar couplings of **1** in the same solvents and same sample composition)[16] was found to be positive. Its magnitude decreases upon heating, reflecting the decrease in the solute ordering power. The dependence of the splitting (in Hz on a logarithmic scale) is plotted in the upper part of Figure 4 (open circles) as a function of the inverse absolute temperature. This dependence could be fitted to an Arrhenius type equation[17,18] (see also Figures SI-2 and SI-3)

$$\Delta\nu_Q^{PBG} = A\exp(-B/T) \quad (1)$$

with

$$A = +396\ \text{Hz} \quad \text{and} \quad B = +205\ \text{K}$$

The corresponding ^{2}H-{^{1}H} 1D spectrum in the chiral PBLG solvent has a quite different behavior (see right column in Figure 3). Below room temperature (<290 K) the spectrum consists of two quadrupolar doublets, whereas above room temperature (>320 K) it has transformed to a single doublet with splittings similar to those observed in the achiral solvent at corresponding temperatures. At around room temperature (290−320 K), the spectrum exhibits characteristic dynamic effects during which the two doublets coalesce.[17,18] The splittings of the inner ($\Delta\nu_Q^{in}$) and outer ($\Delta\nu_Q^{out}$) doublets and of their average ($\Delta\nu_Q^{av}$) at low temperatures, as well as of the coalesced doublet ($\Delta\nu_Q^{coal}$) at high temperatures, are included in the upper part of Figure 4. As for the achiral solvent, the signs of all $\Delta\nu_Q$'s in the PBLG solutions were found to be positive over the whole temperature range. It will be noted that $\Delta\nu_Q^{av}$ and $\Delta\nu_Q^{coal}$ coincide with $\Delta\nu_Q^{PBG}$ (open circles) in the achiral solvent. Evidently, the dynamic process responsible for the coalescence effect in the PBLG solution is different from that observed in the isotropic solvent (Figure 1) and involves a second step of conformational averaging. Moreover, because it is observed in the PBLG solvent and not in PBG, it must involve interchange of chiral species.

At this stage of the analysis we are, however, unable to identify the symmetry of the exchanging species and determine whether the process involves racemization of enantiomeric isomers or interchange of enantiotopic sites in a prochiral molecules. We discuss this point in some detail in a subsequent section. For now we use the spectral data of Figure 3 to derive rate parameters for this process.

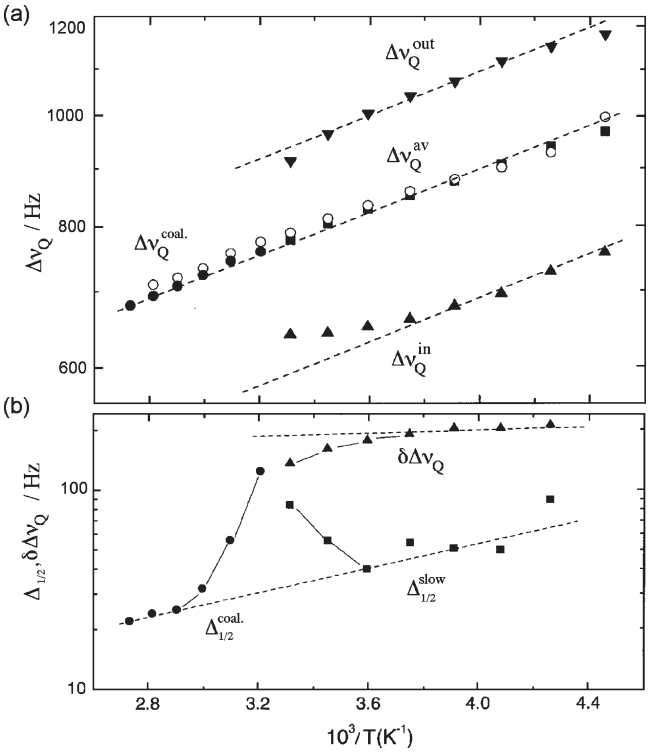

Figure 4. (a) Plots of the quadrupole splittings, $\Delta\nu_Q$, of the aromatic deuterons of **1-d$_4$** dissolved in PBG/$CHCl_3$ (open circles) and in PBLG/$CHCl_3$ (solid symbols) as function of the reciprocal absolute temperature. The triangles (inverted triangles) correspond to $\Delta\nu_Q^{in}$ ($\Delta\nu_Q^{out}$), the squares to the averages, $\Delta\nu_Q^{av} = {}^1/_2(\Delta\nu_Q^{in} + \Delta\nu_Q^{out})$, and the circles to the coalesced, $\Delta\nu_Q^{coal}$, doublets. (b) Corresponding plots for the linewidths, $\Delta_{1/2}$, in the PBLG/$CHCl_3$ solution, below ($\Delta_{1/2}^{slow}$, solid aquares) and above ($\Delta_{1/2}^{coal}$, solid circles) the coalescence temperature. Also plotted (solid triangles) are half the differences, $\delta\Delta\nu_Q = {}^1/_2(\Delta\nu_Q^{out} - \Delta\nu_Q^{in})$, of the outer and inner doublets below coalescence. Note that the vertical scale is logarithmic. The dashed lines were used for inter/extrapolation.

Due to the relatively large natural (dynamic independent) line width, $\Delta\nu_{1/2}^0$, compared with (half) the difference, $\delta\Delta\nu_Q$, of the inner and outer splittings, and the narrow NMR dynamic range (290−320 K) of the process, we choose to use limiting approximate equations for determining its rate (k) in the slow, coalescence, and fast exchange regimes, as follows:[19,20]

$$k_{slow} = \pi(\Delta_{1/2} - \Delta_{1/2}^0) \quad (2)$$

$$k_{coal} = \frac{\pi}{\sqrt{2}}|\delta\Delta\nu_Q| \quad (3)$$

$$k_{fast} = \frac{\pi}{2}\frac{(\delta\Delta\nu_Q)^2}{(\Delta_{1/2} - \Delta_{1/2}^0)} \quad (4)$$

where the $\Delta_{1/2}$'s are the full linewidths at half-maximum height of the measured peaks and $\delta\Delta\nu_Q = {}^1/_2(\Delta\nu_Q^{out} - \Delta\nu_Q^{in})$, both expressed in Hz, while the k's are in s^{-1}.

In the bottom part of Figure 4 are plotted the (average) linewidths, $\Delta_{1/2}$, of the doublet components before and after the coalescence, as well as (half) the difference of the inner and outer splittings, $\delta\Delta\nu_Q$, below the coalescence temperature. For clarity and convenience of the analysis, both the splittings and the linewidths are plotted against the inverse absolute temperature on a semilogarithmic scale (for detailed numerical values see Figures SI-1a and SI-1b). Using these results, with eqs 2−4, the rate constants were derived and drawn as an Arrhenius plot (labeled $C_{2v} \leftrightarrow D_{2h}$) in Figure 5. Also included in this figure is the Arrhenius plot (without the experimental points) for the $C_2 \leftrightarrow C_{2v}$ process obtained from the proton NMR spectra in the isotropic solvent THF.[11]

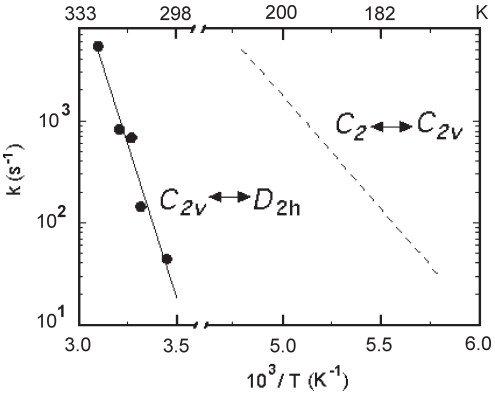

Figure 5. Solid line: Arrhenius plot (with experimental points) for the $C_{2v} \leftrightarrow D_{2h}$ process (290−320 K) derived from the deuterium spectra of **1-d$_4$** dissolved in PBLG/$CHCl_3$ (Figure 3). Dashed line: The Arhenius plot of the $C_2 \leftrightarrow C_{2v}$ process (170−210 K) of **1** dissolved in THF (from ref 11, the experimental points are not shown).

The results, for both processes, were analyzed in terms of the Eyring absolute rate theory (last two terms in eq 5)

$$k = Ae^{-E_a/RT} = \kappa\frac{k_B T}{h}e^{-\Delta G^{\ddagger}/RT} = \kappa\frac{k_B T}{h}e^{-\Delta S^{\ddagger}/R}e^{-\Delta H^{\ddagger}/RT} \quad (5)$$

The definitions of the parameters in this equation and the procedure used in the analysis are as detailed in ref 20 where, as usual, the transmission coefficient κ was taken as unity. The derived kinetic parameters are summarized in Table 1 (note the different sub/superscript used for Arrhenius and Eyring parameters).

The results described above for the chiral PBLG/$CHCl_3$ mesophase at 61.4 MHz were confirmed by measurements at two additional Larmor frequencies, 92.1 and 138.1 MHz (see Figures SI-5 and SI-6). Within the experimental accuracy the line positions and the lineshapes were found to be essentially independent of the magnetic field, as would be expected for spectra dominated by a (first order) quadrupolar interaction (and negligible chemical shift differences). In particular, within the accuracy of the measurements the coalescence temperature, T_{coal}, for the three series of experiments coincided (T_{coal} = 309 ± 4 K) with $\delta\Delta\nu_Q(T_{coal})$ = 170 Hz and k_{coal} = 378 s^{-1}, in agreement with the results in Figure 5.

Additional measurements were performed on solutions of **1-d$_4$** in the chiral mesophase PBLG/DMF, with the much more polar cosolvent than $CHCl_3$. The general behavior of the spectra was similar to that for PBLG/$CHCl_3$ (see Figure SI-7). However, an exact analysis of these results was curbed by their limited dynamic range. From the coalescence temperature, T_{coal} = 318 K, we obtain, $k_{coal} \cong$ 400 s^{-1}, which is close to the value at the corresponding temperature in PBLG/$CHCl_3$, suggesting that the

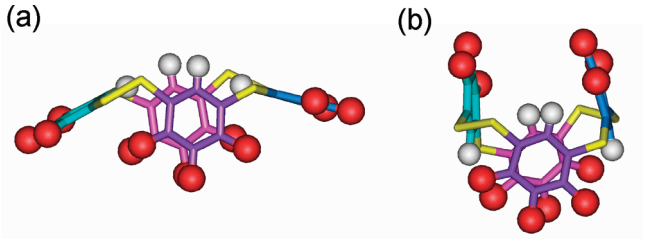

Figure 6. Minimum energy conformations, boat (a) and saddle (b), obtained for **1** by force field (CVFF) calculations. To simplify the presentation the methoxy groups and aromatic hydrogen are drawn as red and white spheres, respectively.

solvent polarity does not significantly affect the conformational dynamics.

3.1c. Nature of the Interconversion Processes in ***1***. The NMR spectra described above provide accurate kinetic data about the low (170−210 K) and high (290−320 K) temperature processes of **1**. However, they are insufficient to provide information on the exact nature of the processes and the conformations involved (except that they contain a C_2 symmetry axis). To aid in the analysis we used force field calculations to search for possible minimum-energy conformations that are consistent with the NMR results. These calculations suggested two main kinds of structures, involving either a boat form with C_2 symmetry or a saddle form with D_2 symmetry, as illustrated in Figure 6.

The relative energies of these two forms are difficult to assess, as they depend delicately on the environment. Thus in vacuum the calculations favor the saddle form (by 15.4 kcal/mol), whereas in the presence of "solvent" (water), the boat appears more stable (by 19.8 kcal/mol). The fact, however, that at low temperature (<170 K) two aromatic and six methoxy lines are observed in the ^{1}H NMR spectrum rules out the D_2 structure as the ground conformation, since in this form all aromatic hydrogens (and respectively the methoxy groups) would be equivalent. We therefore adopt the C_2 symmetry as the low temperature conformation, as before,[10,11] except that its conformation is now taken to be boat-like rather than saddle. As C_2 is a proper group the conformation is optically active and should exhibit a pair of enantiomers.

Low Temperature $C_2 \leftrightarrow C_{2v}$ Interconversion Process. The two aromatic signals observed in the ^{1}H high resolution NMR spectrum at low temperatures (Figure 2) thus correspond to the homotopic pairs (H_8, H_{23}) and (H_{15}, H_{30}), see Figure 1. For consistency with what follows at higher temperatures, we assume that the low temperature process involves exchange between these signals by low amplitude flipping of the benzene rings such that the flatter rings (labeled h) switch upward and the steeper ones (v) flip downward but without crossing the horizontal plane perpendicular to the C_2 axis, as shown schematically in Figure 7a. The middle scheme in this figure shows the conformation obtained after a single up/down flip of the h/v wings. For comparison with the original conformation the transformed conformation is shown again on the right-hand side of the scheme after rotation by $\pi/2$. It evidently corresponds to the mirror image (optical isomer) of the starting conformation, indicating that the process actually corresponds to racemization. In the notation of Figure 7a, the process involves the following hydrogen exchanges

$$h^R \leftrightarrow v^S \quad \text{and} \quad v^R \leftrightarrow h^S \tag{6}$$

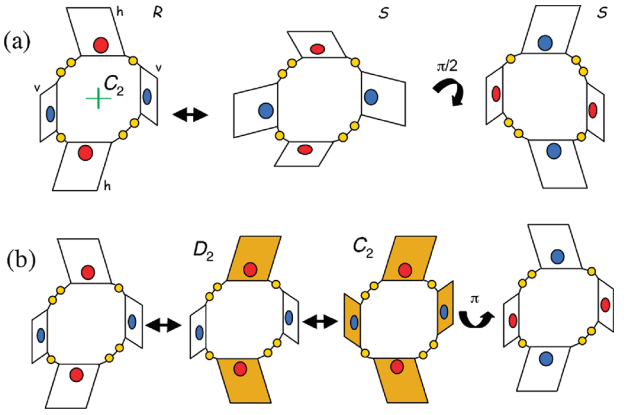

Figure 7. (a) Schematic presentation of the low-temperature $C_2 \leftrightarrow C_{2v}$ process of **1**. The left diagram (starting conformation) is arbitrarily labeled as the R enantiomer. The rhombohedra stand for the more (v) or less (h) tilted benzene rings, and the blue and red circles to their corresponding aromatic hydrogens. The yellow circles indicate sulfur atoms. The double arrow reflects the $C_2 \leftrightarrow C_{2v}$ interconversion. The last diagram obtained by a $\pi/2$ rotation of the center one (about the C_2 axis) shows that the resulting conformer corresponds to the optical isomer (S) of the original one (R). (b) Schematic presentation of the high-temperature $C_{2v} \leftrightarrow D_{2h}$ process of **1**: The first double arrow corresponds to a flip of one pair of benzene rings (shaded) to yield a saddle-like intermediate (with D_2 symmetry). The second double arrow corresponds to a flip of the second pair of benzene rings to complete an umbrella-like inversion. The last diagram is obtained by a π rotation about an in-plane axis passing through the sulfide or disulfide groups, for comparison with the original structure and to show that the process, in fact, interchanges between (on the average) enantiotopic sites.

where h^R (v^S) stand for the hydrogen in the h (v) ring of the R (S) enantiomer. Following Altmann's nomenclature,[21,22] this process belongs to the isodynamic group C_s^v, where $C_s^v = (E, \sigma_v)$, and σ_v is a plane parallel to the C_2 axis. The symmetry of the average molecule (the "Schrödinger supergroup"[21]) then becomes, $C_s^v \otimes C_2 = C_{2v}$. Hence we identify the low temperature process observed in the isotropic solvent as a "$C_2 \leftrightarrow C_{2v}$" process, in which an optically active species becomes "on the average" prochiral with the two pairs of homotopic aromatic hydrogens transforming into two pairs of enantiotopic ones.

High Temperature $C_{2v} \leftrightarrow D_{2h}$ Interconversion Process. Above the coalescence temperature of the $C_2 \leftrightarrow C_{2v}$ process (>220 K), the aromatic hydrogens (and likewise corresponding methoxy groups) are on the average (NMR wise) equivalent. They consist, however, of two (homotopic) pairs of enantiotopic sites (two red and two blue circles in Figure 7). In achiral solvents they all exhibit identical spectra, whereas in chiral solvents they undergo enantiotopic discrimination, as demonstrated for the aromatic deuterons at temperatures below ∼280 K (see right column in Figure 3). The coalescence of the doublets in the latter solvent (at around room temperature) must therefore be associated with a dynamic process that renders the enantiotopic pairs chirally equivalent (homotopic). Such a process corresponds to the flipping of the whole boat through a plane perpendicular to the C_2 axis, like the flipping over of an umbrella. The isodynamic group is then $C_s^h = (E, \sigma_h)$, with the reflection plane, σ_h, perpendicular to the molecular C_2 axis and the symmetry of the "average" molecule becomes, $C_s^h \otimes C_{2v} = D_{2h}$, so that the high-temperature process observed in the CLC solutions corresponds to a "$C_{2v} \leftrightarrow D_{2h}$" interconversion. The process most likely

proceeds in two steps, as depicted in Figure 7b: first a flip of one pair of benzene rings (for example those labeled red) in the starting conformation to yield a saddle intermediate (probably of D_2 symmetry) followed by a flip of the second pair of benzenes thus completing an overall "umbrella inversion" into an inverted boat.

The right diagram is obtained by a π -rotation about an in-plane axis passing through the sulfide (or disulfide) groups. Comparison with the original diagram in the scheme clearly shows that the process involves interchange of (on the average) enantiotopic hydrogens (the red and blue labeled rings in Figure 7b)

$$\mathrm{H(pro\text{-}R)} \leftrightarrow \mathrm{H(pro\text{-}S)} \tag{7}$$

thus rendering the formally enantiotopic pairs homotopic. Evidently the umbrella flipping, involving a saddle intermediate is associated with a higher barrier (28.5 kcal/mol) than the mere one side waving of the "wings" (10.5 kcal/mol; see Table 1). It is likely that above room temperature the population of the intermediate (D_2) saddle form becomes significant and the solute actually consists of a mixture of conformers. However the fast interconversion rates preclude the observation of separate signals for the different conformers in the NMR spectrum.

Origin of the Spectral Enantiodifferentiation. The high temperature process, discussed in the previous section, cannot be detected in achiral solvents since none of the magnetic interactions in compound **1** is modulated by the umbrella-like inversion in such solvents. In chiral solvents discrimination is induced by the selective solute−solvent interaction of the two enantiomers, which is "transferred" to the enantiotopic sites of the "average" prochiral molecule. This is so despite the fact that racemization is fast on the NMR time scale already at much lower temperatures. To understand how this discrimination is brought about we assume, as usual, that it is predominantly caused by the different ordering of the two enantiomers (rather than structural or electronic effects). In the absence of exchange the spectrum of the aromatic deuterons of **1** dissolved in a liquid crystalline solution should consist of two or four quadrupole doublets, depending on whether the solvent is achiral or chiral, each centered about the chemical shifts of the corresponding hydrogen (h or v) in the particular enantiomer (R or S), with intensities proportional to their relative fractional populations, P^{R} and P^{S}. For the boat conformers (C_2 symmetry) the full splitting, $\Delta\nu^i_{\mathrm{Q}}(\mathrm{R/S})$, of the ith deuteron (i = h or v) in the R/S enantiomer is given by[24]

$$\Delta\nu^i_{\mathrm{Q}}(\mathrm{R/S}) = q^i_{aa}S^{\mathrm{R/S}}_{aa} + 1/3(q^i_{bb} - q^i_{cc})(S^{\mathrm{R/S}}_{bb} - S^{\mathrm{R/S}}_{cc}) \tag{8}$$

where $S^{\mathrm{R/S}}_{\alpha\alpha}$ is the elements of the Saupe ordering matrix of the R/S enantiomers and a, b, and c, are their respective principal axes. Also, $q^i_{\alpha\alpha} = {}^3/_4\mathrm{QCC}(3\cos^2\theta^i_\alpha - 1)$, where QCC is the deuterium quadrupole coupling constant in the aromatic C−D bond, assumed to be axially symmetric about the C−D direction (with QCC ≈ 185 kHz) and θ^i_α is the angle between the C−D^i bond direction and the α principal axis of the ordering tensor.

In the very slow regime, in a CLC, we thus expect a spectrum consisting of four doublets, namely two sets of enantiomerically discriminated doublets (see the stick diagram above the horizontal line in Figure 8). This would be the type of spectrum of **1-d$_4$**, had we recorded it in a lyotropic CLC solvent below 170 K. Unfortunately, in this temperature range the PBLG solutions become viscous and gel-like, rendering the NMR spectra unsuitable for quantitative analysis. As we shall see for compound **2**, where the conformational interconversion sets in at much higher temperatures, this is exactly the kind of spectrum observed for this compound at room temperature. For compound **1**, above 210 K the $C_2 \leftrightarrow C_{2v}$ process merges the signals of the two enantiomers as shown schematically by the first coalescence in the bottom part of Figure 8. In particular the signal labeled h$^{\mathrm{R}}$ merges with that of v$^{\mathrm{S}}$ and likewise h$^{\mathrm{S}}$ and v$^{\mathrm{R}}$, resulting in a two-doublet spectrum (green stick diagram in Figure 8) with average splitting

$$\Delta\nu^{\mathrm{r}}_{\mathrm{Q}} = P^{\mathrm{R}}\Delta\nu^{\mathrm{h}}_{\mathrm{Q}}(\mathrm{R}) + P^{\mathrm{S}}\Delta\nu^{\mathrm{v}}_{\mathrm{Q}}(S) = (q^{\mathrm{h}}_{aa}P^{\mathrm{R}}S^{\mathrm{R}}_{aa} + q^{\mathrm{v}}_{aa}P^{\mathrm{S}}S^{\mathrm{S}}_{aa}) + 1/3[(q^{\mathrm{h}}_{bb-cc}P^{\mathrm{R}}S^{\mathrm{R}}_{bb-cc}) + (q^{\mathrm{v}}_{bb-cc}P^{\mathrm{S}}S^{\mathrm{S}}_{bb-cc})] \tag{9a}$$

$$\Delta\nu^{s}_{\mathrm{Q}} = P^{\mathrm{R}}\Delta\nu^{\mathrm{v}}_{\mathrm{Q}}(\mathrm{R}) + P^{\mathrm{S}}\Delta\nu^{\mathrm{h}}_{\mathrm{Q}}(S) = (q^{\mathrm{v}}_{aa}P^{\mathrm{R}}S^{\mathrm{R}}_{aa} + q^{\mathrm{h}}_{aa}P^{\mathrm{S}}S^{\mathrm{S}}_{aa}) + 1/3[(q^{\mathrm{v}}_{bb-cc}P^{R}S^{\mathrm{R}}_{bb-cc}) + (q^{\mathrm{h}}_{bb-cc}P^{\mathrm{S}}S^{\mathrm{S}}_{bb-cc})] \tag{9b}$$

where, for simplicity, we define $q^i_{bb-cc} = q^i_{bb} - q^i_{cc}$ and $S^{\mathrm{R/S}}_{bb-cc} = S^{\mathrm{R/S}}_{bb} - S^{\mathrm{R/S}}_{cc}$. The two doublets, r and s, are now of equal intensities, each centered about its corresponding (weighted) average chemical shifts, $\nu^{\mathrm{r}} = P^{\mathrm{R}}\nu^{\mathrm{h,R}} + P^{\mathrm{S}}\nu^{\mathrm{v,S}}$ and $\nu^{s} = P^{\mathrm{R}}\nu^{\mathrm{v,R}} + P^{\mathrm{S}}\nu^{\mathrm{h,S}}$, where $\nu^{i,K}$ is the chemical shift of the i's hydrogen in the K's enantiomer. This situation corresponds to the experimental spectra of **1** (right-hand side of Figure 3) at temperatures below the setting-in of the high temperature process (<290 K), with the superscripts in and out corresponding to r and s (or vise versa). The discrimination of the two doublets appear as if it emerge from a pair of enantiotopic sites in a prochiral molecule with C_{2v} symmetry. In fact, the spectra correspond to blended signals of the h and v hydrogens and the discrimination reflects the different ordering (and different population) of the enantiomers. From eqs 9a and 9b, it is given by

$$|\delta\Delta\nu_{\mathrm{Q}}| = |\Delta\nu^{\mathrm{out}}_{\mathrm{Q}} - \Delta\nu^{\mathrm{in}}_{\mathrm{Q}}| = |(q^{\mathrm{h}}_{aa} - q^{\mathrm{v}}_{aa})(P^{\mathrm{R}}S^{\mathrm{R}}_{aa} - P^{\mathrm{S}}S^{\mathrm{S}}_{aa}) + 1/3(q^{\mathrm{h}}_{bb-cc} - q^{\mathrm{v}}_{bb-cc})(P^{\mathrm{R}}S^{\mathrm{R}}_{bb-cc} - P^{\mathrm{S}}S^{\mathrm{S}}_{bb-cc})| \tag{10}$$

and assuming $P^{\mathrm{R}} = P^{\mathrm{S}} = 1/2$ yields

$$|\delta\Delta\nu_{\mathrm{Q}}| = \left|\frac{1}{2}(q^{\mathrm{h}}_{aa} - q^{\mathrm{v}}_{aa})(S^{\mathrm{R}}_{aa} - S^{\mathrm{S}}_{aa}) + \frac{1}{6}(q^{\mathrm{h}}_{bb-cc} - q^{\mathrm{v}}_{bb-cc})(S^{\mathrm{R}}_{bb-cc} - S^{\mathrm{S}}_{bb-cc})\right| \tag{11}$$

Since we are unable to associate the measured average splittings ($\Delta\nu^{\mathrm{in/out}}_{\mathrm{Q}}$) with the $\Delta\nu^{\mathrm{r/s}}_{\mathrm{Q}}$ we only define the absolute value of $\delta\Delta\nu_{\mathrm{Q}}$ in eqs 10 and 11. The near temperature independence of $\delta\Delta\nu_{\mathrm{Q}}$ or rather the similar slopes of $\Delta\nu^{\mathrm{out}}_{\mathrm{Q}}$ and $\Delta\nu^{\mathrm{in}}_{\mathrm{Q}}$ below room temperature (Figure 4) indicates that the various $S^{\mathrm{R/S}}_{\alpha\alpha}$'s have similar temperature dependencies.

The high temperature process, corresponding to the umbrella flipping and referred to as the $C_{2v} \leftrightarrow D_{2h}$, in Figure 8, leads to the merging of the $\Delta\nu^{\mathrm{r}}_{\mathrm{Q}}$ and $\Delta\nu^{\mathrm{s}}_{\mathrm{Q}}$ (or $\Delta\nu^{\mathrm{out}}_{\mathrm{Q}}$ and $\Delta\nu^{\mathrm{in}}_{\mathrm{Q}}$) doublets and yielding, in the fast exchange regime (above ∼300 K), a single doublet with average splitting of

$$\langle\Delta\nu_{\mathrm{Q}}\rangle = 1/2(\Delta\nu^{\mathrm{r}}_{\mathrm{Q}} + \Delta\nu^{s}_{\mathrm{Q}}) = 1/2\{(q^{\mathrm{h}}_{aa} + q^{\mathrm{v}}_{aa})(P^{\mathrm{R}}S^{\mathrm{R}}_{aa} + P^{\mathrm{S}}S^{\mathrm{S}}_{aa}) + 1/3[(q^{\mathrm{h}}_{bb-cc} + q^{\mathrm{v}}_{bb-cc})(P^{\mathrm{R}}S^{\mathrm{R}}_{bb-cc} + P^{\mathrm{S}}S^{\mathrm{S}}_{bb-cc})]\} \tag{12}$$

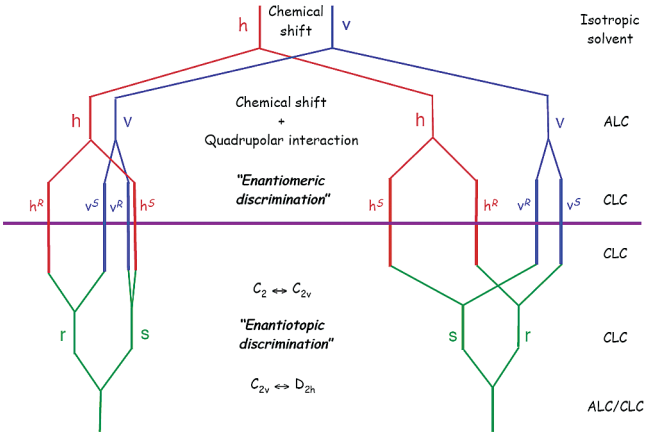

Figure 8. Hierarchy of spectral splitting of the aromatic deuterium NMR of **1-d$_4$** in liquid crystalline solutions and its coalescence by dynamic processes. The top pair of lines represent the h (red) and v (blue) deuterons in the rigid molecule separated by their respective chemical shifts. The next level shows the effect of quadrupolar interaction in an achiral liquid crystalline solvent (ALC), followed by enantiomeric discrimination in a CLC (above and below the center solid line). The first coalescence below the center line is due to the $C_2 \leftrightarrow C_{2v}$ process. The diagram shows its effect in CLC, where the h and v sites merge into the (effective) homotopic r and s (green) pair. In ALC it would yield the stick diagram shown in the bottom (single doublet). The second averaging is due to the $C_{2v} \leftrightarrow D_{2h}$ process and can only be observed in chiral solvents. Equal populations of enantiomers and same sign of quadrupole interaction for all deuterons is assumed. A somewhat exaggerated chemical shift (compared to the quadrupole splitting) is used to emphasize the origin of the spectrum asymmetry in the slow exchange regime.

It is the same type of spectrum observed in ALC above the coalescence range of the $C_2 \leftrightarrow C_{2v}$ process (Figure 3, left)

$$\Delta\nu_Q^r = \Delta\nu_Q^s = \Delta\nu_Q = 1/2[(q_{aa}^v + q_{aa}^h)S_{aa} + 1/3(q_{bb-cc}^v + q_{bb-cc}^h)S_{bb-cc}] \quad (13)$$

This equation matches eq 12, by setting, $S_{\alpha\beta}^R = S_{\alpha\beta}^S$, $= S_{\alpha\beta}$ and $P^R = P^R = 1/2$, as expected for an ALC.

We have thus demonstrated that the NMR spectra (^{1}H in isotropic solvents and ^{2}H in CLC) of the hexathiametacyclophane, **1**, can be explained in terms of a succession of two chiral averaging processes, which we labeled $C_2 \leftrightarrow C_{2v}$ and $C_{2v} \leftrightarrow D_{2h}$. We proposed mechanisms for these rearrangement processes (Figure 7) and their rate parameters were determined (Table 1). There is little that can be done with the experimental data concerning the ordering of the conformers without additional measurements, since, even if their exact geometry (and hence the $q_{\alpha\alpha}^i$'s) were known, there are still three independent parameters to be determined for each enantiomer while only a limited number of splittings is available.

3.2. Metacyclophane 2. *3.2a. Proton NMR Spectrum in Isotropic Solvents and the Kinetic Analysis of the Dynamic Process.* The proton NMR spectrum of **2** in perdeuterated nitrobenzene was first reported by Pappalardo and Bottino in 1984.[10] Because of the low solubility of the compound and the low sensitivity of their spectrometer (90 MHz) the spectrum was only recorded at 423 K, yielding a singlet at 6.65 ppm (relative intensity 1) due to the aromatic hydrogens and two methyl peaks at 2.29 ppm (3) and 1.98 ppm (6). On this basis they concluded that the conformation of **2** is that of a rigid crown, with (according to their drawing) D_2 symmetry. With today's modern NMR spectrometers we were able to record its spectrum in saturated solutions at room temperature in several solvents (including chloroform, pyridine, and nitrobenzene). These room temperature spectra are quite different from that reported by Pappalardo and are consistent with a molecule possessing a 2-fold symmetry. The spectra are slightly solvent and temperature dependent, and

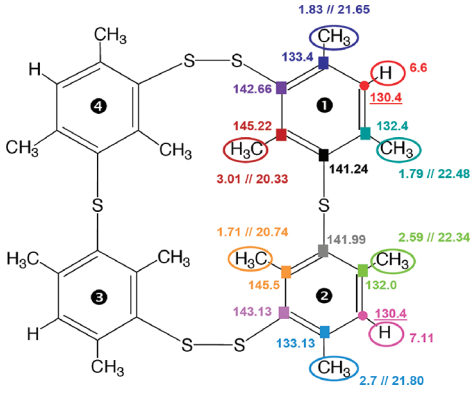

Figure 9. ^{1}H and ^{13}C chemical shifts (values in ppm relative to TMS) for compound **2** dissolved in $CDCl_3$ at 300 K. The assignment was made using ^{1}H−^{13}C HSQC and HMBC 2D corrélation experiments.

consist of two aromatic peaks in the range 6.5−7.5 ppm (each of relative intensity 1) and two sets of triplets, in the range 1.5−3.5 ppm (3) due to the methyl groups. A more complete analysis, including ^{13}C spectra, was performed in chloroform using HSQC and HMBC 2D correlation experiments. The resulting ^{1}H and ^{13}C chemical shifts are summarized in Figure 9.

It is thus clear that between room temperature and 423 K compound **2** undergoes a conformational rearrangement process on the NMR time scale. Under this assumption the present results are consistent with those of Pappalardo.[10] To study the kinetics of this process, we used the high temperature boiling solvent nitrobenzene and recorded the solute spectrum up to 413 K. Selected spectra are shown in the upper traces of Figure 10 [note that in this solvent two of the high-field methyl peaks accidentally overlap (see bottom trace in the figure)]. Above about 360 K, line broadening sets in characteristic of a dynamic process that leads to coalescence of the aromatic peaks and pairwise of the methyl signals. The exchanging pairs were identified by a 2D exchange experiment as indicated by common

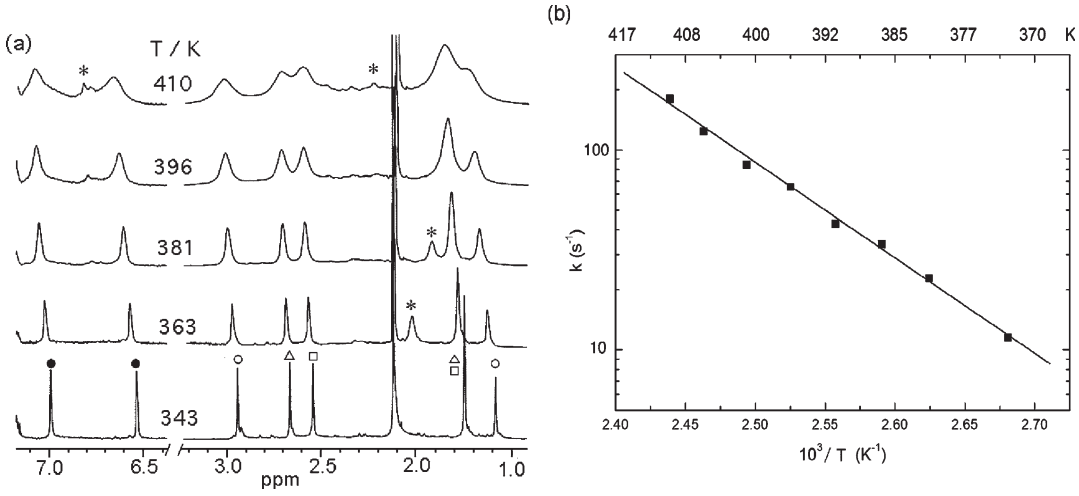

Figure 10. (a) ^{1}H NMR spectra (500 MHz) of **2** in perdeuterated nitrobenzene at different temperatures, as indicated. The common symbols on the bottom spectrum indicate mutually exchanging peaks. The asterisks mark impurity signals. (b) An Arrhenius plot derived from spectra of the type shown on the left.

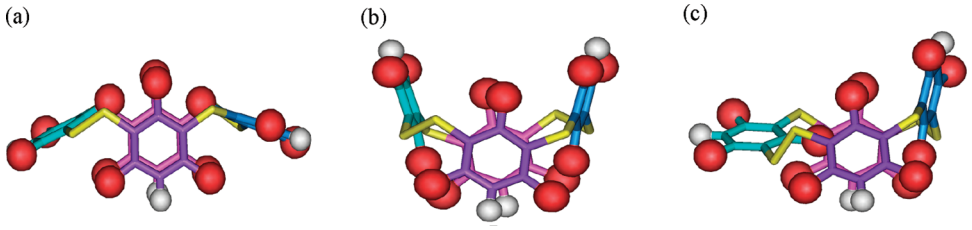

Figure 11. Conformations of compound **2**, derived from force field calculations. (a) An unstable boat form; (b) the ground state, slightly twisted, crown conformation with C_2 symmetry; (c) a local minimum crown-boat conformation that could serve as intermediate in the crown inversion. The red and white balls represent methoxy groups and hydrogen atoms, respectively. The yellow bars stand for sulfide bonds.

symbols on the 343 K trace of the figure. The temperature dependent spectra were analyzed in terms of a two site jump process, using the slow exchange approximation (eq 2). An Arrhenius plot of the result, as shown on the right-hand side of Figure 10, yielded the following kinetic parameters, $A = 6.2 \times 10^{13}$ s^{-1}, $E_a = 21.4$ kcal/mol, $\Delta H^{\ddagger} = 20.6$ kcal/mol, and $\Delta S^{\ddagger} = 2.0$ cal/mol K.

3.2b. Low Energy Conformations of ***2*** *and the Nature of the Dynamic Process.* For compound **2** we are confronted again with the situation of having accurate data on the rate parameters of the conformational rearrangement, but little experimental information on its structure and on the mechanism of the rearrangement. As for **1**, we resort to force field calculations. It turns out that the substitution pattern of the methyl groups around this cyclophane tetramer strongly affects the energies of its various conformations. In particular the calculations indicate that a boat form (see Figure 11a), which was found to be the most stable one for compound **1**, is highly unstable and rapidly converts to a crown conformation, as shown by the central structure in the figure. Such a minimum energy structure with a C_2 symmetry axis in which the benzene rings pointing up, say 1 and 3, are not symmetry related to the rings 2 and 4, pointing down (for example by being differently inclined to the C_2 axis), is consistent with the above ^{1}H NMR results (two aromatic and six methoxy signals). The calculations also indicate a half crown−half boat conformation with a high but locally minimum energy (right structure in the figure) that may serve as an intermediate in interconversion processes.

With such a crown structure for the ground conformation of **2**, two dynamic processes may be envisioned as leading to the broadening (and coalescence) of the ^{1}H NMR spectra in Figure 10. In the first process, a, the pairs of (homotopic) benzene rings (related by the C_2 axis) 1, 3 and 2, 4, interchange their inclination relative to C_2, but without overall flipping of the crown. The process thus corresponds (isodynamic group) to a C_2 flip about an axis perpendicular to the molecular C_2 axis. In the fast exchange this leads to a spin Hamiltonian with an average (Schrödinger Supergroup) $C_2(z) \otimes C_2(\sigma) = D_2$ symmetry,[21] where $C_2(z)$ and $C_2(\sigma)$ stand for the groups, (E, $C_{2\parallel}$) and (E, $C_{2\perp}$), respectively. The process may thus be classified as "$C_2 \leftrightarrow D_2$" and is schematically drawn in Figure 12a. Note that it differs from the low temperature reaction of **1**, in particular it does not correspond to racemization, but rather individual rearrangement of each enantiomer, with exchanges of the type

$$1^R \leftrightarrow 2^R \quad \text{and} \quad 1^S \leftrightarrow 2^S \tag{14}$$

This can readily be seen by noting that an in-plane π-flip (say about an axis connecting the bisulfide groups) of the rearranged molecule restores the original structure, but with the sites 1 and 2 (1′ and 2′) interchanged. In principle, this mechanism may be followed at higher temperatures by an inversion process as described below for process b. In this, altenative, mechanism the averaging of the two pairs of wings involves complete inversion of the

crown, with the up-pointing benzene rings flipping down and vice versa. This corresponds to a $C_2 \leftrightarrow D_{2h}$ process and is schematically drawn in Figure 12b. The "average" molecule is now achiral and all aromatic sites are homotopic. No chiral discrimination is therefore expected in the fast limit regime of this mechanism.

The activation energy measured for **2** (21.4 kcal/mol) is close to that of the high temperature process of **1** (28.5 kcal/mol) and more than twice that for the low temperature one (10.5 kcal/mol). This may suggest that the dynamic process measured in **2** corresponds to the inversion reaction (b). However we cannot be sure, especially since the substitution patterns in the two compounds is quite different. In principle a distinction between the alternative mechanisms could be made by examining the dynamic spectra in a chiral environment. In the slow exchange, enantiomeric discrimination will result in four sets of subspectra, two for the *R* and two for the *S* enantiomers. For the first mechanism, (a), the four sets of spectra will pairwise merge (according to eq 14), resulting in, in the fast exchange limit, an enantiomerically discriminated pair of subspectra. In contrast, mechanism (b) will lead to merging of all four subspectra, yielding, in the fast exchange limit, a single spectrum due to the different homotopically (on the average) related sites.

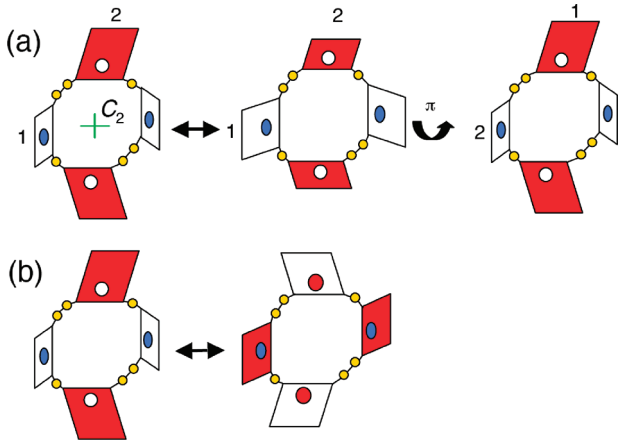

Figure 12. Possible mechanisms for the process leading to the dynamic NMR line broadening in Figure 10. (a) The $C_2 \leftrightarrow D_2$ interconversion process, where rings 1, 3 and 2, 4 interchange their orientation relative to the C_2 axis (without overall flipping of the crown structure). The last diagram results from a π flip about an in-plane axis connecting the sulfide (or disulfide) groups. It shows that the process does not involve racemization. (b) The $C_2 \leftrightarrow D_{2h}$ interconversion process with the upper pair of rings flipping down and vice versa. Note that the benzene ring inclinations are now (on the average) the same.

We were hoping to distinguish between these possibilities using deuterium NMR of **2-d$_4$** (compound **2** deuterated in the unsubstituted aromatic sites) dissolved in our CLC solvents. However, experimental restrictions (limited solubility and limited temperature range of our deuterium probes) prevented us from carrying out the experiments. In the next paragraph we describe the deuterium spectrum of **2-d$_4$** dissolved in PBG/$CHCl_3$ and PBLG/$CHCl_3$ and explain how, in principle (in the absence of the above limitations), an identification of the rearrangement mechanism could be made.

3.2c. ^2H-{^1H} NMR Spectra in ALC and CLC Solvents. Examples of proton-decoupled 1D and 2D deuterium NMR spectra (92.1 MHz, using a cryoprobe) of **2-d$_4$** in the achiral (PBG/$CHCl_3$) and chiral (PBLG/$CHCl_3$) solvents (at 330 K) are shown in Figure 13. The 2D patterns on the right correspond to tilted *Q*-COSY spectra, while those on the left to their respective 1D projections. In the ALC solvent two doublets (labeled 1 and 2) due to the nonequivalent aromatic hydrogens, are observed. The asymmetry in the spectrum reflects their different chemical shifts, which match well those measured for the aromatic hydrogens in the isotopically normal compound (Figure 10). In the CLC

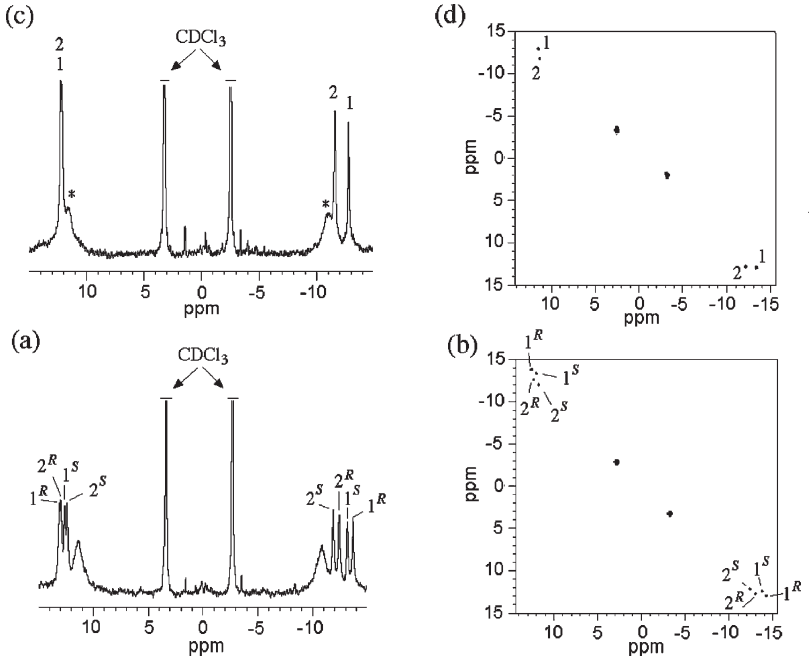

Figure 13. 92.1 MHz ^2H-{^1H} NMR spectra of **2-d$_4$** recorded in PBLG/$CHCl_3$ (a and b) and PBG/$CHCl_3$ (c and d) solvents at 330 K. On the right are displayed the 2D *Q*-COSY Fz spectra, while on the left are their corresponding 1D tilted projections. The asterisk marks the doublet ($\Delta\nu_Q \approx 2060$ Hz) due to the NAD signal of the PBLG benzyl side groups[23] The numbers 1 and 2 label the (more or less shielded) aromatic deuterons, and R and S the two enantiomers. Note that the labels 1^R, 1^S (2^R, 2^S) are arbitrary.

Table 2. Chemical Shifts (δ) and Quadrupolar Splittings ($\Delta\nu_Q$) of the Aromatic Deuterons of 2-d_4 Dissolved in PBG/$CHCl_3$ and PBLG/$CHCl_3$ at 330 K

parameters	PBG/$CHCl_3$		PBLG/$CHCl_3$			
δ/ppm	6.70	7.05	6.70		7.05	
$\Delta\nu_Q$/Hz	2303	2181	2464	2405	2307	2232
$\Delta\nu_Q$ ($CDCl_3$)/Hz[a]	531		560			

[a] Corresponds to the NAD signal of the chloroform cosolvent.

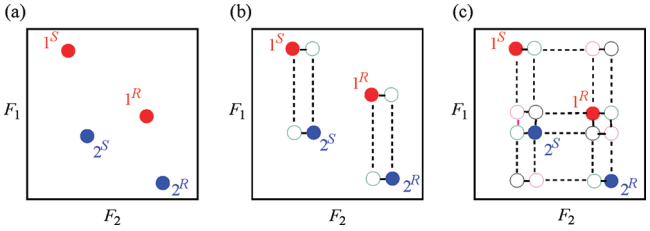

Figure 14. Schematic representation of the cross-peak patterns expected for the deuterium 2D exchange spectrum of **2-d_4** under different conditions. A pattern similar to that of the bottom right corner of Figure 13b is considered and an identical sign for all $\Delta\nu_Q$'s is assumed. (a) In the absence of exchange: only the diagonal peaks (red for 1 and blue for 2) are observed. (b) The cross-peaks pattern (open circles) expected for the $C_2 \leftrightarrow D_2$ process. (c) Same as in (b) for the $C_2 \leftrightarrow D_{2h}$ (crown inversion) process.

solvent, each quadrupolar doublet splits into two due to chiral discrimination. The spectra are thus consistent with (although they do not provide a proof for) the adopted crown structure with C_2 symmetry for the compound. The doubling of the spectrum in CLC reflects spectral enantiodiscrimination, but we cannot associate pair of lines to a particular enantiomer. The labeling 1^R, 1^S (2^R, 2^S) is therefore arbitrary (each pair is interchangeable). The observed spectra thus correspond to the stick diagrams labeled respectively ALC and CLC, above the center line in Figure 8. (with 1, 2 instead of v, h). The chemical shift and the quadrupole splitting of the aromatic deuterons, in both solvents are summarized in Table 2. A similar pattern of splittings is also observed for the methoxy deuterons in **2-d_{36}** (compound **2** deuterated in the methoxy groups) in the two solvents. However the extent of the chiral discrimination is smaller and the corresponding splittings not well resolved.

The kind of spectrum exhibited by **2-d_4** in the PBLG/$CHCl_3$ mesophase is ideally suited for studying the mechanism of its conformational rearrangement as discussed in the previous section, in particular whether it follows the $C_2 \leftrightarrow D_2$ or the $C_2 \leftrightarrow D_{2h}$ process. The working range of our deuterium cryoprobe (required for recording the spectra of the weekly soluble **2-d_4**) is, however, limited to 350 K, which is far below the on-set range of dynamic line broadening (above 370 K for protons and considerably higher for deuterons, see Figure 10). The same restriction even precludes the possibility of observing cross peaks in 2D exchange experiments. From Figure 10 the estimated lifetime of the rearrangement process at 330 K is ~2 s, (~0.5 s at 350 K), whereas the deuterium T_1 in this temperature range is about 30 ms, much too short to allow exchange cross peaks to be observed. Indeed a deuterium Zeeman 2D exchange (EXSY) experiment[25] performed at 330 K with mixing times ranging from 0.01 to 100 ms did not reveal any such peaks. Measurements at much higher temperatures (>400 K) are required to observe exchange cross peaks in such experiments.

To demonstrate the different effects that processes (a) and (b) may exhibit on dynamic NMR spectra we depict in Figure 14 schematic diagrams of 2D exchange patterns. For simplicity identical signs are assumed for all $\Delta\nu_Q$'s and only a single set of peaks (similar to that in the bottom right corner of Figure 13b) is considered. In the absence of exchange only the diagonal peaks are observed (Figure 14a). The first $C_2 \leftrightarrow D_2$ process (eq 14) interchanges the 1^R and 2^R (1^S and 2^S) deuterons, leading to the cross peaks pattern as in Figure 14b, whereas the crown inversion process, $C_2 \leftrightarrow D_{2h}$, mixes all diagonal peaks as depicted in the last diagram of the figure. Hence, in principle, the mechanisms are readily distinguishable.

4. CONCLUSIONS

The structural and dynamic properties of the macrocyclic cyclophanes depend strongly on the number, size, and nature of their substituents. In the present paper we used NMR spectroscopy to study two derivatives of the 18-membered dodecamethoxy hexathia metacyclophane: (**1**) with the inner benzene sites unsubstituted and (**2**) with the inner sites substituted with a methyl groups. While **2** is essentially rigid at room temperature and only exhibits dynamic effects at temperatures well above 370 K, **1** is highly flexible and undergoes two types of conformational interconversion already below room temperature. These consist of a low-activation energy (10.5 kcal/mol), one-sided, ring flipping of the ground state boat structure, followed by an umbrella like inversion of the boat, with a considerably higher activation barrier (28.5 kcal/mol).

The identification of the ground state conformers and the nature of the dynamic processes are difficult to assess from the NMR spectra alone due to the small number of accessible magnetic parameters in these compounds. We therefore combine molecular force field calculations with NMR measurements in achiral isotropic and CLC solutions. The application of the latter method is useful in several respects: (i) It helps to identify the symmetry of the species and (ii) in certain cases it makes it possible to measure dynamic processes that are, otherwise, undetectable. For the analysis of the results we used the concept of average symmetry of flexible molecules.[21] Even though no molecule with such an average structure actually exists, the concept allows an easy analysis of the spectra and facilitates the characterization of the interconversion process. In the case of flexible optically active compounds undergoing rapid racemization, the average structure often corresponds to a prochiral molecule. The NMR spectra in chiral solvents may then exhibit effective enantiotopic discrimination and can reveal dynamic effects which are unobservable in achiral solvents.

In the present study compound **1** was found to exhibit two types of interconversion symmetries, successively transforming the ground symmetry of the molecule from C_2 to C_{2v} and then to D_{2h}, with the last one only observable in chiral solvents. Compound **2** also exhibits conformational rearrangement, but only at well above room temperature. Because of experimental limitations we could only study its dynamic in achiral isotropic solvents but not in our CLC's. The exact mechanism of its interconversion process remains therefore, so far, unsolved.

■ ASSOCIATED CONTENT

Supporting Information. Figures SI-1 to SI-6 with corresponding tables. This material is available free of charge via the Internet at http://pubs.acs.org.

■ AUTHOR INFORMATION

Corresponding Author
*E-mail: philippe.lesot@u-psud.fr; Zeev.Luz@weizmann.ac.il.

■ ACKNOWLEDGMENT

P.L. thanks CNRS for its constant financial support. Financial support from the TGI-RMN THC FR3050 at Lyon for conducting of part of this research is also gratefully acknowledged. Z.L. acknowledges the historic generosity of the Harold Perlman Family to the Weizmann Institute. We thank Miri Eisenstein for the CVFF calculations and Leonid Konstantinovski for help in recording and analyzing ^{1}H NMR spectra.

■ REFERENCES

(1) Ernst, L. *Prog. Nucl. Magn. Reson. Spectrosc.* **2000**, *37*, 47.
(2) Lesot, P.; Aroulanda, C.; Luz, Z. *J. Chem. Phys.* **2009**, *131*, 104501.
(3) Aroulanda, C.; Merlet, D.; Courtieu, J.; Lesot, P. *J. Am. Chem. Soc.* **2001**, *123*, 12059.
(4) Lesot, P.; Merlet, D.; Sarfati, M.; Courtieu, J.; Zimmermann, H.; Luz, Z. *J. Am. Chem. Soc.* **2002**, *124*, 10071.
(5) Lafon, O.; Lesot, P.; Zimmermann, H.; Poupko, R.; Luz, Z. *J. Phys. Chem. B* **2007**, *111*, 9453.
(6) Aroulanda, C.; Merlet, D.; Courtieu, J.; Lesot, P. *J. Am. Chem. Soc.* **2001**, *123*, 12059.
(7) Lesot, P.; Lafon, O.; Courtieu, J.; Berdagué, P. *Chem.—Eur. J.* **2004**, *10*, 3741.
(8) Lesot, P.; Courtieu, J. *Prog. Nucl. Magn. Reson, Spectrosc.* **2009**, *55*, 128.
(9) Bresciani-Pahor, N.; Calligaris, M.; Randaccio, L.; Bottino, F.; Pappalardo, S. *Gazz. Chim. Ital.* **1988**, *110*, 227.
(10) Pappalardo, S.; Bottino, F.; Ronsisvalle, G. *Phosphorus Sulfur* **1984**, *19*, 327.
(11) Zimmermann, H.; Poupko, R.; Luz, Z. *Tetrahedron* **1988**, *44*, 277.
(12) Sarfati, M.; Lesot, P.; Merlet, D.; Courtieu, J. *Chem. Commun.* **2000**, 2069.
(13) Lafon, O.; Lesot, P.; Zimmermann, H.; Poupko, R.; Luz, Z. *J. Phys. Chem. B* **2007**, *111*, 9453.
(14) Dauber-Osguthorpe, P.; Roberts, V. A.; Osguthorpe, D. J.; Wolff, J.; Genest, M.; Hagler, A. T. *Proteins: Struct., Funct., Genet.* **1988**, *4*, 31.
(15) *Gaussian 03*; Gaussian Inc.: Pittsburgh, PA, 2003. *Gaussian 03*, revision C.02; Gaussian, Inc.: Wallingford, CT, 2004.
(16) Emsley, J. W.; Lesot, P.; D. Merlet, D. *Phys. Chem. Chem. Phys.* **2004**, *6*, 522.
(17) Lesot, P.; Lafon, O.; Kagan, H. B.; Fan, C.-A. *Chem. Commun.* **2006**, *4*, 389.
(18) Lafon, O.; Lesot, P.; Fan, C.-A.; Kagan, H. B. *Chem.—Eur. J.* **2007**, *13*, 3772.
(19) Sandstrom, J. *Dynamic NMR Spectroscopy*; Academic Press: London, 1982; Chapter 2.
(20) Martin, M. L.; Delpuech, J.-J.; Martin, G. J. *Practical NMR spectroscopy*; Heyden & Son Ltd.: London, 1980.
(21) Altmann, S. L. *Proc. R. Soc. London* **1967**, *A298*, 184.
(22) Lesot, P.; Lafon, O.; Zimmermann, H.; Luz, Z. J. *Am. Chem. Soc.* **2008**, *130*, 8754.
(23) Lesot, P.; Lafon, O.; Aroulanda, C.; Dong, R. *Chem.—Eur. J.* **2008**, *14*, 4082.
(24) Emsley, J. W.; Lindon, J. C. *NMR Spectroscopy Using Liquid Crystal Solvents*; Pergamon Press: Oxford, U.K., 1975; Chapter 1.
(25) Boeffel, C; Luz, Z.; Poupko, R; Vega, A., J. *Israel J. Chem.* **1988**, *28*, 283.